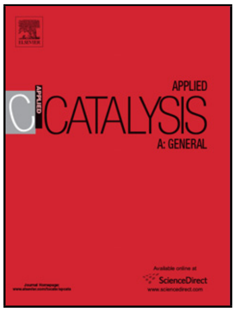

Title: Oxidative dehydrogenation of but-1-ene with lattice oxygen in ferrite catalysts

Authors: Takayasu Kiyokawa, Naoki Ikenaga

PII: S0926-860X(17)30049-2
DOI: http://dx.doi.org/doi:10.1016/j.apcata.2017.02.004
Reference: APCATA 16140

To appear in: *Applied Catalysis A: General*

Received date: 12-10-2016
Revised date: 14-12-2016
Accepted date: 3-2-2017

Please cite this article as: Takayasu Kiyokawa, Naoki Ikenaga, Oxidative dehydrogenation of but-1-ene with lattice oxygen in ferrite catalysts, Applied Catalysis A, General http://dx.doi.org/10.1016/j.apcata.2017.02.004

# Oxidative dehydrogenation of but-1-ene with lattice oxygen in ferrite catalysts

Takayasu Kiyokawa[*], Naoki Ikenaga[*]

Graduate School of Science and Engineering, Kansai University, 3-3-35 Yamate, Suita, Osaka 564-8680, Japan

[*]Corresponding author: Takayasu Kiyokawa, Naoki Ikenaga

E-mail addresses: k452360@kansai-u.ac.jp (T. Kiyokawa), ikenaga@kansai-u.ac.jp (N. Ikenaga)

Tel.: +81-6-6368-0894

Fax.: +81-6-6388-8869

## Key words

Ferrite; But-1-ene; Buta-1,3-diene; Oxidative dehydrogenation, Lattice oxygen

## Graphical abstract

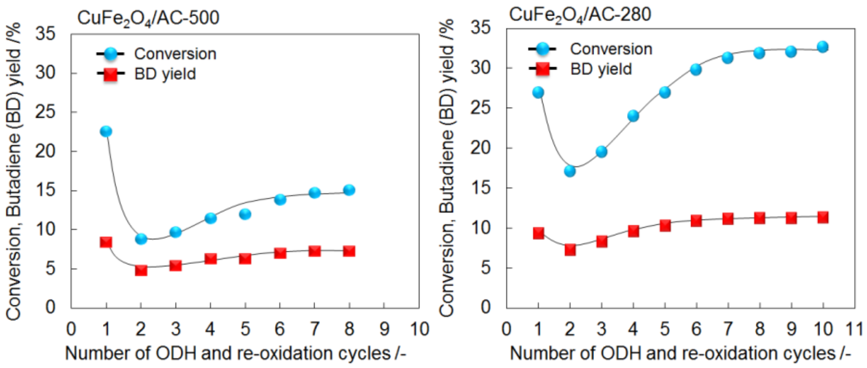

**Highlights**

1. $CuFe_2O_4$/AC catalyst produced BD with oxidative dehydrogenation of but-1-ene at a lower temperature.
2. The lattice oxygen of Cu-O was used for the ODH and was recovered by molecular $O_2$.
3. $CuFe_2O_4$/AC maintained the BD yield during repeated ODH.

## Abstract

The oxidative dehydrogenation (ODH) of but-1-ene was carried out using the lattice oxygen in ferrite catalysts in the temperature range of 200-300 °C with a fixed-bed flow reactor at atmospheric pressure. Various ferrite catalysts, such as $NiFe_2O_4$/AC-500, $ZnFe_2O_4$/AC-500, $CoFe_2O_4$/AC-500, and $CuFe_2O_4$/AC-500, -400, -300, -280, were prepared in the presence of activated carbon in the calcination temperature range of 280-500 °C. When but-1-ene-TPR was measured using various ferrite catalysts, $CuFe_2O_4$/AC-500 progressed the ODH of but-1-ene at 200-300 °C. Among the catalysts, $CuFe_2O_4$/AC-500 showed the highest Buta-1,3-diene (BD) yield, at 270 °C. XRD and XPS analyses of the catalyst after the ODH suggested that the lattice oxygen in Cu-O bonded to the tetrahedral site ($Cu^{2+}{}_T$) of the ferrite structure was used for the ODH. In addition, the used catalyst was recovered by re-oxidation with molecular $O_2$. Moreover, $CuFe_2O_4$/AC-280, which calcined at 280 °C, had the highest specific surface area and improved the BD yield with an increase in contact area with but-1-ene. In the repeated ODH (reaction and regeneration cycle), $CuFe_2O_4$/AC-500 and -280 catalysts maintained BD yields of 7.5% and 11.3%, respectively. BD production is thought to be related to the amount of $Cu^{2+}{}_T$.

## 1. Introduction

Buta-1,3-diene (BD) has attracted interest as a monomer of petrochemical products such as polybutadiene rubber, styrene butadiene rubber, and ABS resin. About 90% of BD is produced by purifying C4 fraction such as BD, n-butene, and n-butane obtained from the endothermic steam-cracking of naphtha. However, this process produces many petrochemicals such as ethylene and propylene at the same time and needs a temperature more than 700 °C. Therefore, this process consumes a lot of energy and can not produce BD efficiently. However, this process produces many petrochemicals such as ethylene, propylene at the same time. Therefore, this process consumes a lot of energy and can not produce BD efficiently.

Recently, oxidative dehydrogenation (ODH) of the C4 fraction with molecular $O_2$ (Eq. (1)) has attracted attention from the perspective of energy saving, because it is an exothermic process and can more efficiently produce BD at a lower temperature than the current process. Moreover, since this is single process only to produce BD, BD can be produced with high selectivity without by-products such as ethylene and propylene. Moreover, because this process is single process only to produce BD, BD is produced high selectively without byproducts such as ethylene, propylene.

$$1\text{-}C_4H_8\ (g) + 1/2O_2\ (g) \rightarrow C_4H_6\ (g) + H_2O\ (l)\ \Delta H_{298.15} = -177\ \text{kJ/mol} \qquad (1)$$

Various complex metal oxides and supported catalysts have been investigated for the ODH of many hydrocarbons, such as propane [1], ethylbenzene [2], ethane [3], n-butane [4], and n-butene [5]. For the ODH of n-butene and n-butane, ferrite-type catalysts [5-19], V-containing catalysts [20-22], and Bi-Mo catalysts [23-27] exhibited high activity. It was reported that the Bi-Mo catalyst progressed the ODH through the Mars−van Krevelen mechanism with oxygen mobility and gave high catalytic activity, in which the high BD selectivity, low $CO_2$ selectivity, and the high BD yield, for the ODH of but-1-ene to BD at 440 °C [26]. When the lattice oxygen in the Bi-Mo catalyst was used for the ODH of but-1-ene, BD and a reduced metal oxide catalyst were produced, and then the reduced metal oxide was re-oxidized with molecular $O_2$ to recover the active site in the catalyst [23, 24].

Among these catalysts for the ODH of the C4 fraction, ferrite-type catalysts have been widely studied. Spinel structures, such as Zn-Fe [5-11, 17, 18], Zn-Fe-Cr [13], Zn-Fe-Al [12], and γ-$Fe_2O_3$ [15, 16], showed high activity. However, the presence of α-$Fe_2O_3$ decreased the conversion and the BD selectivity [8]. Among ferrite catalysts, zinc ferrite has been widely investigated. For example, it was reported that a zinc ferrite catalyst that was modified by heteropoly acid or sulfonic acid was effective for the ODH of but-1-ene [9, 10]. In addition, when zinc ferrite was prepared by the co-precipitation method, pH control was important to obtain high but-1-ene conversion and high BD selectivity [11].

The reaction mechanism for the ODH of n-butene with the zinc ferrite catalyst is known to proceed through the Mars−van Krevelen mechanism cycle, the same as that with the Bi-Mo catalyst [7-9]. However, it was proposed that the ferrite-type catalyst was deactivated as a result of an increase in $Fe^{2+}$ produced by reducing $Fe^{3+}$ that was isolated from the spinel phase [18, 19]. In order to maintain high oxygen mobility and inhibit change in the spinel structure, $Sb_2O_4$, $BiPO_4$, or $SnO_2$ as an oxygen donor was added to the zinc ferrite catalyst. These catalysts showed high oxygen mobility and high ODH activity for a long time [17, 18]. On the other hand, the ODH with the zinc ferrite catalyst has been carried out under steam and $O_2$ flow. Because the latent heat of steam is large, a high energy level and a high temperature of 400-450 °C are necessary. Furthermore, because the C4 fraction is highly reactive, the complete oxidation reaction (Eqs. (2), (3)) proceeds easily during the ODH under $O_2$ atmosphere.

$$1\text{-}C_4H_8\ (g) + 6O_2\ (g) \rightarrow 4CO_2\ (g) + 4H_2O\ (l)\ \Delta H_{298.15} = -2717\ \text{kJ/mol} \qquad (2)$$

$$C_4H_6\ (g) + 11/2O_2\ (g) \rightarrow 4CO_2\ (g) + 3H_2O\ (l)\ \Delta H_{298.15} = -2540\ \text{kJ/mol} \qquad (3)$$

Therefore, it was proposed that the lattice oxygen of the V-containing $SiO_2$ catalyst could be used to prevent the complete oxidation of the reactant and the product, and that the catalyst that loses the lattice oxygen can be re-oxidized by introducing molecular $O_2$ after the reaction (Eqs. (4), (5)) [28]. Furthermore, the catalytic activity was maintained throughout repeated ODHs.

$$1\text{-}C_4H_8\,(g) + MO_x\,(s) \rightarrow C_4H_6\,(g) + H_2O\,(l) + MO_{x-1}\,(s) \quad (4)$$

$$MO_{x-1}\,(s) + 1/2O_2\,(g) \rightarrow MO_x\,(s) \quad (5)$$

It is considered that high oxygen mobility of the lattice oxygen in the catalyst at a lower reaction temperature would be the most important factor and would show good catalytic performance for the ODH of the C4 fraction.

Our laboratory, on the other hand, found that ferrite can be prepared at a low temperature, such as 500 $^oC$, in the presence of activated carbon [29].

This study examined the ODH of but-1-ene with the lattice oxygen in various ferrite catalysts prepared with activated carbon. In order to inhibit complete oxidation, the lattice oxygen in the catalyst was used as a mild oxidant, and then the catalytic activity of the ferrite catalyst for the ODH of but-1-ene was investigated.

## 2. Experimental

### 2.1 Materials

$Fe(NO_3)_3{\cdot}9H_2O$ (assay = min. 99.0%), $Ni(NO_3)_2{\cdot}6H_2O$ (assay = 99.0%), $Zn(NO_3)_2{\cdot}6H_2O$ (assay = 99.0%), $Co(NO_3)_2{\cdot}6H_2O$ (assay = 98.0%), $Cu(NO_3)_2{\cdot}3H_2O$ (assay = min. 99.0%), and activated carbon (AC) were purchased from Wako Pure Chemical Industry and were used for the preparation of ferrite catalysts. But-1-ene ($1\text{-}C_4H_8$) (assay = min. 99.0%) was supplied from Sumitomo Seika Chemical.

### 2.2 Catalyst preparation

### Preparation by impregnation method

Various ferrite catalysts were prepared by the impregnation method. AC was impregnated with a mixed aqueous solution of $Fe(NO_3)_3{\cdot}9H_2O$ and $Ni(NO_3)_2{\cdot}6H_2O$, $Zn(NO_3)_2{\cdot}6H_2O$, $Co(NO_3)_2{\cdot}6H_2O$, or $Cu(NO_3)_2{\cdot}3H_2O$ as Ni, Zn, Co, or Cu:Fe=1:2 in molar ratio. After the mixture was allowed to stand at room temperature overnight, excess water was evaporated to dryness under reduced pressure. The solid was then dried at 70 $^{o}$C overnight in vacuo. Nickel, zinc, and cobalt ferrites were calcined at 500 $^{o}$C for 2 h in air. Copper ferrite was calcined at 280-500 $^{o}$C for 2 h in air. CuO was prepared in same method at 500 $^{o}$C. Hereafter, the notation is $NiFe_2O_4$/AC-500, $ZnFe_2O_4$/AC-500, $CoFe_2O_4$/AC-500, $CuFe_2O_4$/AC-280, -300, -400, -500, and CuO/AC.

## 2.3 Catalyst test

### ODH of but-1-ene using lattice oxygen in ferrite catalyst

The ODH of but-1-ene was carried out using a fixed-bed flow quartz reactor at various temperatures under atmospheric pressure. After 200 mg of the catalyst was placed in the reactor, 5 mL/min of but-1-ene and 25 mL/min of Ar were introduced for 8 min. The re-oxidation after ODH was performed under 5 mL/min of $O_2$ and 25 mL/min of Ar for 8 min at the same temperature as reaction temperature. The relative error of the experimental operation is within 5 %.

The C4 fractions (1-$C_4H_8$, *cis*-2-$C_4H_8$, *trans*-2- $C_4H_8$, and $C_4H_6$) were analyzed by a flame ionization detector (FID) gas chromatograph (Shimadzu GC14B, column: Unicarbon A-400). CO and $CO_2$ were also analyzed by the FID gas chromatograph (column: Activated carbon) equipped with a methanizer (Shimadzu MTN-1). $H_2$ was analyzed by a thermal conductivity detector (TCD) gas chromatograph (Shimadzu

GC8A, column: Activated carbon).

## 2.4 Catalyst characterization

X-ray diffraction (XRD) patterns were obtained by the powder method with a Shimadzu XRD-6000 diffractometer using monochromatic CuKα radiation. X-ray photoelectron spectra (XPS) analyses were carried out with a JEOL model JPS-9010MX using MgKα radiation as an energy source. The surface area of the catalyst was measured by the Brunauer–Emmett–Teller (BET) method at 77 K using $N_2$ as an adsorbate with a MicrotracBEL (BELSORP-mini II-ISP). Thermogravimetry and differential thermal analysis (TG-DTA) (Shimadzu DTG-60) was used to measure the burning point of AC. The reactor was heated to 800 $^{o}$C at a rate of 10 $^{o}$C /min under 100 mL/min of air and was maintained at 800 $^{o}$C for 10 min. A temperature-programmed reaction of but-1-ene (1-$C_4H_8$-TPR) was carried out under but-1-ene/Ar=5/25 mL/min using a fixed-bed flow reactor in which 200 mg of catalyst was placed. As water removal, the catalyst was pretreated at 200 $^{o}$C under an Ar atmosphere, and then the reactor was heated to 500 $^{o}$C at a rate of 5 $^{o}$C/min under but-1-ene and Ar flow. The products ($H_2$, $H_2O$, $C_4H_6$, $CO_2$) were continuously analyzed by a Q-mass mass spectrometer (Hiden Analytical, HAL 201) fitted with an outlet of the reactor.

## 3. Results and Discussion

### 3.1 Activity test of various ferrite catalysts by 1-$C_4H_8$-TPR measurement

1-$C_4H_8$-TPR was measured in order to confirm the lattice oxygen mobility of ferrite catalysts such as $NiFe_2O_4$/AC-500, $ZnFe_2O_4$/AC-500, $CoFe_2O_4$/AC-500, and $CuFe_2O_4$/AC-500. The results are shown in Fig. 1. Since $H_2O$ and $CO_2$ were seen at 380

$^{o}$C, $NiFe_2O_4$/AC-500 progressed the complete oxidation of but-1-ene. At about 400 $^{o}$C, $NiFe_2O_4$/AC-500 progressed the decomposition of but-1-ene to produce $H_2$. The formation of $CO_2$ increased from about 460 $^{o}$C. However, the production of $H_2O$ was not seen. Therefore, carbon produced by the decomposition of but-1-ene seemed to be oxidized by the lattice oxygen (Fig. 1 a)). On the other hand, $CoFe_2O_{4/}$AC-500 and $ZnFe_2O_4$/AC-500 produced BD, although the latter produced BD and $H_2$ at over 400 $^{o}$C. Since $H_2O$ was not observed, this catalyst progressed the simple dehydrogenation of but-1-ene (Fig. 1 b)). $CoFe_2O_4$/AC-500 catalyst produced BD, $H_2O$, $CO_2$, and $H_2$ at over 400 $^{o}$C. Therefore, this catalyst proceeded to the ODH, the complete oxidation, and the simple dehydrogenation of but-1-ene at the same time (Fig. 1 c)). When $CuFe_2O_4$/AC-500 was used to measure 1-$C_4H_8$-TPR, BD and $H_2O$ were produced at over about 200 $^{o}$C (Fig. 1 d)). At 300 $^{o}$C, $CO_2$ and $H_2O$ were formed with the complete oxidation of but-1-ene. Since $H_2$ formed at over 400 $^{o}$C, the decomposition of but-1-ene progressed. These results indicate that $CuFe_2O_4$/AC-500 catalyst is the most suitable for ODH at a lower temperature. Since $CuFe_2O_4$/AC-500 produced $CO_2$ at 300 $^{o}$C and $H_2$ at 400 $^{o}$C, the ODH using $CuFe_2O_4$/AC-500 was carried out at a temperature range of 200-300 $^{o}$C.

### 3.2 Effect of reaction temperature on ODH with lattice oxygen of $CuFe_2O_4$/AC-500

The ODHs with lattice oxygen of $CuFe_2O_4$/AC-500 were carried out at 200-300 $^{o}$C. The results are illustrated in Fig. 2. When the ODH was conducted at 200 $^{o}$C, $CuFe_2O_4$/AC-500 indicated the highest conversion, of 25.6%, with the isomerization reaction. However, low BD selectivity of 17.9% and low BD yield of 4.6% were obtained. In the ODHs at 250-270 $^{o}$C, this catalyst exhibited higher conversion, BD selectivity, and BD yield. At 270 $^{o}$C, $CuFe_2O_4$/AC-500 gave a conversion of 21.3%, high BD selectivity of 39.9%, and the highest BD yield, 8.5%. At 300 $^{o}$C, this catalyst showed low conversion of 12.8% as the isomerization reaction declined, high $CO_2$ selectivity of 14.2%, and a low yield of 6.5%. Since the catalyst gave the highest BD yield at 270 $^{o}$C, 270 $^{o}$C was the most suitable reaction temperature for the ODH with $CuFe_2O_4$/AC-500.

XRD analyses were carried out to examine the change in the crystallite structure of the catalyst before and after the ODH and after the re-oxidation at 270 $^{o}$C. XRD patterns are shown in Fig. 3. $CuFe_2O_4$ and CuO diffraction peaks were seen in $CuFe_2O_4$/AC-500 before the ODH (Fig. 3a)). $CuFe_2O_4$/AC-500 after the reaction exhibited diffraction peaks of metal copper in addition to copper ferrite, and CuO diffraction peak was clearly decreased as compared to that of the fresh catalyst (Fig. 3b)). The lattice oxygen in CuO may also be used for the ODH of but-1-ene. In order to confirm the reactivity of the lattice oxygen, CuO/AC catalyst was used for the ODH of but-1-ene. When the CuO/AC was used for the ODH, CuO indicated the lower conversion of 1.9 %, the higher $CO_2$ selectivity of 36.9 %, and the lower BD yield of 0.9 % than those of $CuFe_2O_4$/AC catalyst. In other words, the reducibility of the lattice oxygen in CuO is very low. Therefore, it is suggested that the lattice oxygen in $CuFe_2O_4$ is more effective than that of CuO for the ODH. After the re-oxidation, $CuFe_2O_4$ and CuO diffraction peaks were similar to those of the catalyst before the reaction. Furthermore, since the crystallite sizes of $CuFe_2O_4$ in $CuFe_2O_4$/AC-500 before and after the reaction calculated by the Scherrer equation were 8.8 nm and 10.4 nm, respectively (Fig. 3c)), the $CuFe_2O_4$ crystallite barely grew. Therefore, the crystal structure in the used $CuFe_2O_4$/AC-500 could be recovered by re-oxidation.

To investigate the active species for the ODH with $CuFe_2O_4$/AC-500 and the change in valence values of iron and copper oxide species, XPS analyses were used for $CuFe_2O_4$/AC-500 before and after the reaction at 270 $^{o}$C. XPS spectra of Fe and Cu species are shown in Fig. 4. In general, the XPS spectra of Fe and Cu species of $CuFe_2O_4$ can be divided into two peaks, such as octahedral and tetrahedral sites [30, 31]. $Fe^{3+}$ species related to tetrahedral ($Fe^{3+}{}_{T}$) and octahedral ($Fe^{3+}{}_{O}$) sites appear at 713.6 and 710.5 eV, respectively. $Cu^{2+}$ species related to tetrahedral ($Cu^{2+}{}_{T}$) and octahedral ($Cu^{2+}{}_{O}$) sites appear at 935.8 and 934.1 eV, respectively. XPS spectra of $CuFe_2O_4$/AC-500 before the reaction indicated $Fe^{3+}$ and $Cu^{2+}$ were related to tetrahedral and octahedral sites, respectively (Fig. 4 a), b)). According to the XPS analysis of $CuFe_2O_4$/AC-500 after the ODH, because XPS spectra of reduced Fe species were not observed in the catalyst after the reaction, lattice oxygen in the Fe-O bond was not used for the ODH (Fig. 4 a)).

On the other hand, $Cu^0$ appeared at 932.1 eV in addition to two peaks with $Cu^{2+}$ related to tetrahedral and octahedral sites in the catalyst after the reaction (Fig. 4 b)). Moreover, $Cu^{2+}{}_{T}$ in $CuFe_2O_4$/AC-500 catalyst clearly decreased after the ODH. XPS spectrum of $CuFe_2O_4$/AC-500 after the re-oxidation showed $Cu^{2+}{}_{T}$ in addition to $Cu^{2+}{}_{O}$, similar to those of the catalyst before the reaction. Therefore, oxygen species bonded to $Cu^{2+}{}_{T}$ would be used as active sites for the ODH of but-1-ene. Iron oxide species did not relate to the ODH. However, it is thought that the iron species is necessary to form $Cu^{2+}{}_{T}$ by combining Fe and Cu. The ODH of but-1-ene to BD was promoted by forming $Cu^{2+}{}_{T}$. The atomic ratio of Cu and O on $CuFe_2O_4$/AC-500 surface before and after the reaction and after the re-oxidation calculated from XPS analyses are shown in Table 1. Although Cu species/O atomic ratio (b)) on the catalyst surface after the ODH was increased from 0.37 to 0.46 as compared to that (a)) of fresh catalyst. For the catalyst after the re-oxidation, Cu species/O ratio was decreased from 0.46 to 0.4 as compared to that of the catalyst after the ODH. As indicated in Fig. 4, the change in the valence value of Fe species was not seen. Therefore, the lattice oxygen on only copper oxide species can be used for the ODH of but-1-ene, and the used lattice oxygen can be regenerated by the re-oxidation. According to the results of XRD and XPS analyses, because the used $CuFe_2O_4$/AC-500 catalyst could be regenerated by re-oxidation with oxygen, the re-oxidized $CuFe_2O_4$/AC-500 can be used for the ODH of but-1-ene again.

### 3.3 Effect of calcination temperature on ODH

The effects of the specific surface area and the crystallite size of $CuFe_2O_4$ in $CuFe_2O_4$/AC-500 catalyst with a change in the calcination temperature on the ODH were examined.

In order to confirm the burning point of AC, TG-DTA measurement of $CuFe_2O_4$/AC before calcination was carried out. The results are illustrated in Fig. 5. Remarkable weight loss and increased DTA were observed at 300 $^{o}$C with burning AC. Therefore, $CuFe_2O_4$/AC catalysts were calcined at 280-500 $^{o}$C. Their XRD patterns are shown in Fig. 6, and the specific surface area and crystallite size are shown in Table 2. $CuFe_2O_4$ diffraction peaks were observed for all catalysts (Fig. 6 a)-d)). Therefore, it is considered that the crystal structure of $CuFe_2O_4$ would be formed by AC burning, because no DTA increase or weight gain, which are related to the formation of iron and copper oxide after AC burning, was seen (Fig. 5). On the other hand, the specific surface area increased in the order of $CuFe_2O_4$/AC-280>300>400>500=105>76>59>34 $m^2/g$ and the crystallite size tended to decrease in the order of $CuFe_2O_4$/AC-280<300<400<500=6.8<7.4<8.1<8.8 nm as the calcination temperature decreased (Table 2). When the catalyst was calcined at 280 $^{o}$C, it showed a higher specific surface area of 105 $m^2$/g and a smaller crystallite size of 6.8 nm compared to those of catalysts calcined at other temperatures.

The effects of the calcination temperature on the ODH are shown in Fig. 7. $CuFe_2O_4$/AC-400 and $CuFe_2O_4$/AC-500 gave quite similar BD yields of about 8.5%. $CuFe_2O_4$/AC-300 showed a higher conversion, 24.4%, and a higher BD yield, 8.8%. When the ODH was carried out using $CuFe_2O_4$/AC-280, conversion of 27.6% and a BD yield of 9.2% were obtained. $CuFe_2O_4$/AC, which has a high specific surface area, tended to give a high BD yield because of the larger contact area with but-1-ene.

### 3.4 Evaluation of activity maintenance for repeated ODH

ODHs and re-oxidation were repeated using $CuFe_2O_4$/AC-500 and $CuFe_2O_4$/AC-280. The results are shown in Figs. 8 and 9, respectively. For $CuFe_2O_4$/AC-500 (Fig. 8), the second reaction gave a lower conversion, 8.8% and a lower BD yield, 4.7%, and higher $CO_2$ selectivity, 11.3%, than those of the first reaction. The increase in the $CO_2$ selectivity after the second ODH indicated that the complete oxidation of C4 fraction such as but-1-ene and BD progressed. Thereafter, the conversion and the BD selectivity gradually increased from third to eighth ODH. After the seventh ODH, lower conversion of 15%, BD yield of 7.5%, higher BD selectivity of 48.2%, and $CO_2$ selectivity of 4.2% were maintained. The BD yield stabilized at the eighth ODH, and $CuFe_2O_4$/AC-500 stably produced BD in the repeated ODH. When $CuFe_2O_4$/AC-280 was used for the repeated ODH (Fig. 9), in the second ODH, the conversion decreased from 26.9% to 17%, similar to that of $CuFe_2O_4$/AC-500. Even at the tenth ODH, the conversion increased from 26.9% to 32.6% with the isomerization reaction, BD selectivity of about 35% was maintained, and $CO_2$ selectivity decreased relative to that at the second ODH. The BD yield then increased from 9.3% to 11.3%.

To examine the change in the crystal structure during the repeated ODHs, XRD analyses of $CuFe_2O_4$/AC-500 and -280 were carried out after the repeated ODHs. The XRD patterns are shown in Fig. 10.

CuO diffraction peaks in both catalysts after the repeated ODHs were larger than those before the reaction (Fig. 10 a), b)). However, as already mentioned in section 3.2, since CuO/AC showed the lower conversion, the high $CO_2$ selectivity, and the low BD yield, the results after the second ODH (Figs. 8, 9) show that $CuFe_2O_4$ produced by liberated Cu species from the spinel phase inhibited the complete oxidation of but-1-ene and encouraged the isomerization reaction.

In order to evaluate the effects of Cu species such as tetrahedral and octahedral sites on the repeated ODHs, XPS analyses were used for the $CuFe_2O_4$/AC-500 and -280 after the repeated ODHs. The ratios of $Cu^{2+}{}_T/Cu^{2+}{}_O$ calculated from XPS analyses are shown in Table 3. The ratio of $Cu^{2+}{}_T/ Cu^{2+}{}_O$ of $CuFe_2O_4$/AC-500 after the first ODH was lower than that of the fresh catalyst (Table 3 a), b)), but the $Cu^{2+}{}_T/ Cu^{2+}{}_O$ ratio after the eighth ODH was higher than that after the first re-oxidation (Table 3 b), c)). Therefore, the BD yield gradually recovered and stabilized at the eighth ODH. The $Cu^{2+}{}_T/ Cu^{2+}{}_O$ ratio in $CuFe_2O_4$/AC-280 after the first re-oxidation was lower than that of the fresh catalyst (Table 3 d), e)). However, the $Cu^{2+}{}_T/ Cu^{2+}{}_O$ ratio after the tenth ODH increased from 0.26 to 0.36 compared to the fresh catalyst (Table 3 d), f)). These results suggested that an increase in the BD yield is related to the amount of $Cu^{2+}{}_T$ phase. Therefore, although the role of $Cu^{2+}{}_T$ phase is not clear, its existence might be the most important factor for BD production in the ODH of but-1-ene.

## 4. Conclusion

$CuFe_2O_4$/AC-500 gave a BD yield of 8.5% at 270 $^{o}$C, and the used catalyst was regenerated by re-oxidation with molecular $O_2$. The results of XRD and XPS analyses of $CuFe_2O_4$/AC-500 after the ODH showed that the ODH progressed by using the lattice oxygen of Cu-O bonded in $Cu^{2+}{}_T$. The $CuFe_2O_4$/AC catalyst that had a higher specific surface area was more efficient for the ODH, and $CuFe_2O_4$/AC-280, which had the highest specific surface area, 105 $m^2$/g, gave the highest BD yield, 9.3%.

For the repeated ODHs using $CuFe_2O_4$/AC-500 and $CuFe_2O_4$/AC-280, $CuFe_2O_4$/AC-500 maintained a BD yield of about 8% until the eighth ODH. When $CuFe_2O_4$/AC-280 was used for the repeated ODHs, BD was formed until the tenth ODH and the BD yield increased from 9.5% to 11.3%. From the XRD and XPS analyses of $CuFe_2O_4$/AC-500 and $CuFe_2O_4$/AC-280 after the repeated ODHs, the generation of CuO is involved in the inhibition of complete oxidation of but-1-ene. In addition, the increase in $Cu^{2+}{}_T$ phase seemed to increase the BD yield in the ODH of but-1-en.

## 5. References

[1] F. Ma, S. Chem, Y. Li, H. Zhou, A. Xu, W. Lu, Appl. Surf. Sci., **313** (2014) 654-659

[2] H. Fan, J. Feng, X. Li, Y. Guo, W. Li, K. Xie, Chem. Eng. Sci., **135** (2015) 403-411

[3] I.A. Bakare, S.A. Mohamed, S. Al-Ghamdi, S.A. Razzak, M.M. Hossain, H.I. de Lasa, Chem. Eng. J., **278** (2015) 207-216

[4] M. Setnicka, R. Bulanek, L. Capek, P. Cicmanec, J. Mol. Catal., **344** (2011) 1-10

[5] J.A. Toledo, N. Nava, M. Martinez, X. Bokhimi, Appl. Catal. A: Gen., **234** (2002) 137-144

[6] H. Armendariz, G. Aguilar-Rios, P. Salas, M.A. Valenzuela, I. Schifter, H. Arriola,

N. Nava, Appl. Catal. A: Gen., **92** (1992) 29-38

[7] H. Lee, J.C. Jung, H. Kim, Y.M. Chung, T.J. Kim, S.J. Lee, S.H. Oh, Y.S. Kim, I.K. Song, Catal. Lett., **131** (2009) 344-349

[8] Y.M. Chung, Y.T. Kwon, T.J. Kim, S.J. Lee, S.H. Oh, Catal. Lett., **130** (2009) 417-423

[9] H. Lee, J.C. Jung, I.K. Song, Catal. Lett., **133** (2009) 321-327

[10] H. Lee, J.C. Jung, H. Kim, Y.M. Chung, T.J. Kim, S.J. Lee, S.H. Oh, Y.S. Kim, I.K. Song, Korean J. Chem. Eng., **26** (2009) 994-998

[11] H. Lee, J.C. Jung, H. Kim, Y.M. Chung, T.J. Kim, S.J. Lee, S.H. Oh, Y.S. Kim, I.K. Song, Catal. Commun., **9** (2008) 1137-1142

[12] J.A. Toledo, P. Bosch, M.A. Valenzuela, A. Montoya, N. Nava, J. Mol. Catal., **125** (1997) 53-62

[13] H. Armendariz, J.A. Toledo, G. Aguilar-Rios, M.A. Valenzuela, P. Salas, A. Cabral, H. Jimenez, I. Schifter, J. Mol. Catal., **92** (1994) 325-332

[14] R.J. Rennard, W.L. Kehl, J. Catal., **21** (1971) 282-293

[15] B.J. Liaw, D.S. Cheng, B.L. Yang, J. Catal., **118** (1989) 312-326

[16] W.Q. Xu, Y.G. Yin, G.Y. Li, S. Chen, Appl. Catal. A: Gen., **89** (1992) 131-142

[17] F.Y. Qiu, L.T. Weng, E. Sham, P. Ruiz, B. Delmon, Appl. Catal., **51** (1989) 235-253

[18] Y.M. Chung, Y.T. Kwon, T.J. Kim, S.J. Lee, S.H. Oh, Catal. Lett., **131** (2009) 579-586

[19] M.A. Gibson, J.W. Hightower, J. Catal., **41** (1976) 431-439

[20] A. Dejoz, J.M. LoÂpez Nieto, F. MaÂrquez, M.I. VaÂzquez, Appl. Catal. A. Gen., **180** (1999) 83-94

[21] J.K. Lee, H. Lee, U.G. Hong, J. Lee, Y.-J. Cho, Y. Yoo, H.S. Jang, I.K. Song, J.

Ind. Eng. Chem., **18** (2012) 1096-1101

[22] J.M. Lopez Nieto, P. Concepci, A. Dejoz, H. Knozinger, F. Melo, M.I. Vazquez., J. Catal., **189** (2000) 147–157

[23] J.H. Park, H. Noh, J.W. Park, K. Row, K.D. Jung, C.-H. Shin, Appl. Catal. A. Gen., **431** (2012) 137-143

[24] J.C. Jung, H. Lee, H. Kim, Y.M. Chung, T.J. Kim, S.J. Lee, S.H. Oh, Y.S. Kim, I.K. Song, Catal. Commun., **9** (2008) 943–949

[25] J.C. Jung, H. Kim, Y.M. Chung, T.J. Kim, S.J. Lee, S.H. Oh, Y.S. Kim, I.K. Song, J. Mol. Catal., **264** (2007) 237-240

[26] J.C. Jung, H. Kim, Y.M. Chung, T.J. Kim, S.J. Lee, S.H. Oh, Y.S. Kim, I.K. Song, Appl. Catal. A: Gen., **317** (2007) 244-249

[27] A.P.V. Soares, L.D. Dimitrov, M.C.A. Oliveira, L. Hilaire, M.F. Portela, R.K. Grasselli, Appl. Catal. A: Gen., **253** (2003) 191-200

[28] K. Fukudome, N. Ikenaga, T. Miyakke, T. Suzuki, Catal. Sci. Technol., **1** (2011) 987-998

[29] N. Ikenaga, N. Chiyoda, H. Matsushima, T. Suzuki, Fuel, **81** (2002) 1569-1576

[30] Y. Wang, H. Zhao, M. Li, J. Fan, G. Zhao., Appl. Catal. B: Environ., **147** (2014) 534-545

[31] C. Reitz, C. Suchomski, J. Haetge, T. Leichtweiss, Z. Jaglicic, I. Djerdj, T Brezesinski, Chem. Commun., **48** (2012) 4471-4473

## 6. Acknowledgment

This research was financially supported in part by the Kansai University Grant-in-Aid for progress of research in graduate course, 2016

# Justification for Publication

This manuscript exceeds the default character count described in the author guidelines, but this original manuscript contains very significant results and discussions required to clarify the specific and excellent effects of the design of an attractive ferrite catalyst that can produce BD at a lower reaction temperature than was used in other studies on the ODH of but-1-ene.

Table 1 Cu and O atomic ratio of $CuFe_2O_4$/AC-500 catalyst before and after ODH and after re-oxidation calculated from XPS analysis

| | Fresh, used, and re-oxidized catalysts | $Cu^{2+,0}/O$ |
|---|---|---|
| a) | $CuFe_2O_4$/AC-500 fresh | 0.37 |
| b) | $CuFe_2O_4$/AC-500 after ODH | 0.46 |
| c) | $CuFe_2O_4$/AC-500 after re-oxidation | 0.40 |

Table 2 Specific surface area and crystallite size of $CuFe_2O_4$/AC catalyst prepared at different calcination temperatures

| Sample | Specific surface area ($m^2$/g) | Crystallite size (nm) |
|---|---|---|
| $CuFe_2O_4$/AC-500 | 34 | 8.8 |
| $CuFe_2O_4$/AC-400 | 59 | 8.1 |
| $CuFe_2O_4$/AC-300 | 76 | 7.4 |
| $CuFe_2O_4$/AC-280 | 105 | 6.8 |

Table 3 $Cu^{2+}_{T}/Cu^{2+}_{O}$ ratio of $CuFe_2O_4$/AC catalyst before and after ODH calculated from XPS analysis

| | Fresh and used catalyst | $Cu^{2+}_{T}$ (%) | $Cu^{2+}_{O}$ (%) | $Cu^{2+}_{T}/Cu^{2+}_{O}$ |
|---|---|---|---|---|
| a) | $CuFe_2O_4$/AC-500 fresh | 20.5 | 79.5 | 0.26 |
| b) | $CuFe_2O_4$/AC-500 after first re-oxidation | 17.9 | 82.1 | 0.22 |
| c) | $CuFe_2O_4$/AC-500 after eighth ODH | 20.2 | 79.8 | 0.25 |
| d) | $CuFe_2O_4$/AC-280 fresh | 20.8 | 79.2 | 0.26 |
| e) | $CuFe_2O_4$/AC-280 after first re-oxidation | 18.4 | 81.6 | 0.23 |
| f) | $CuFe_2O_4$/AC-280 after tenth ODH | 26.7 | 73.3 | 0.36 |

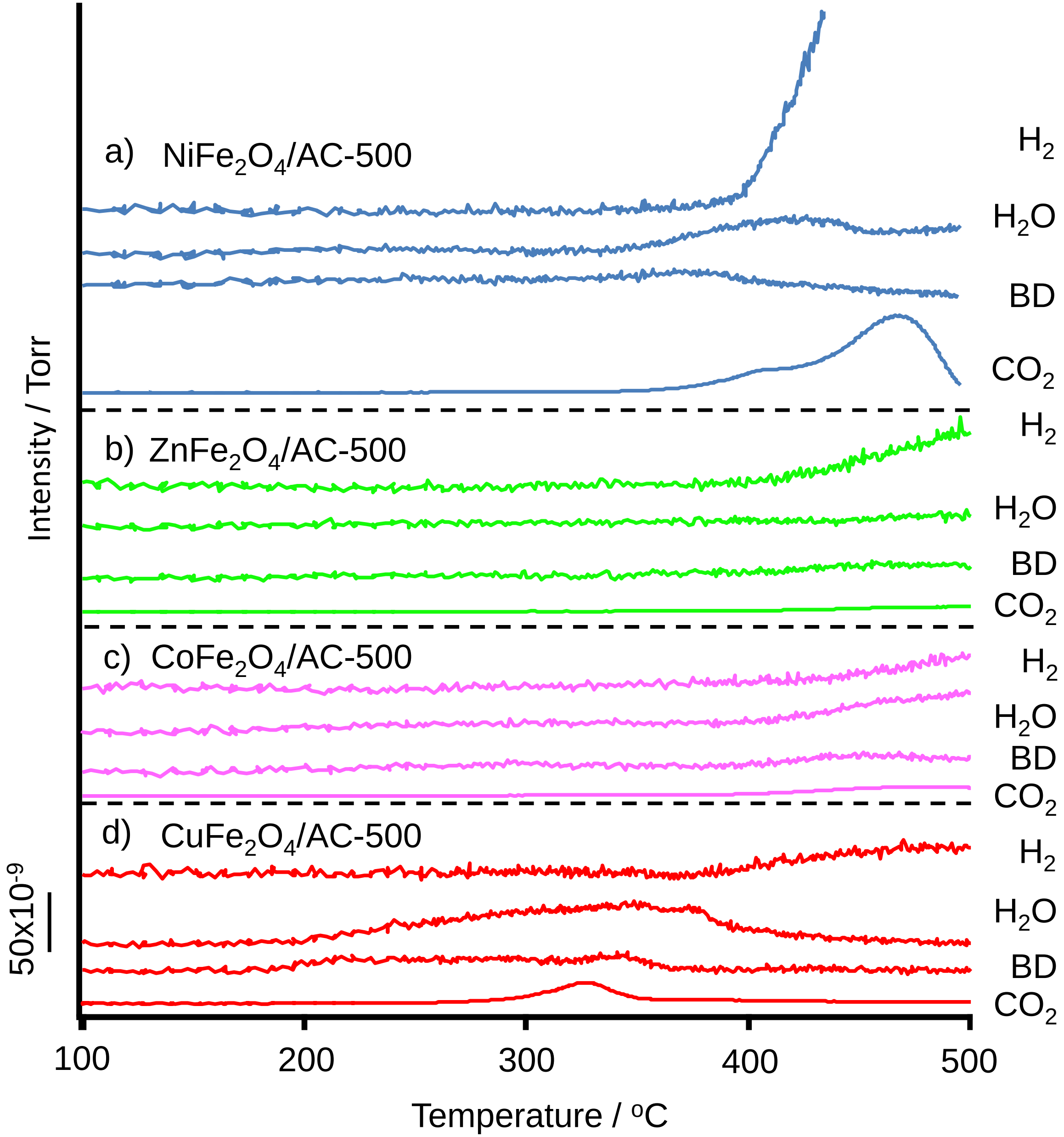

Fig.1 But-1-ene-TPR profiles with various ferrite catalysts
Catalyst weight: 200 mg, 1-$C_4H_8$=/Ar=25/5 mL/min, heating ratio: 5 °C/min,
a) $NiFe_2O_4$/AC-500, b) $ZnFe_2O_4$/AC-500, c) $CoFe_2O_4$/AC-500, d) $CuFe_2O_4$/AC-500

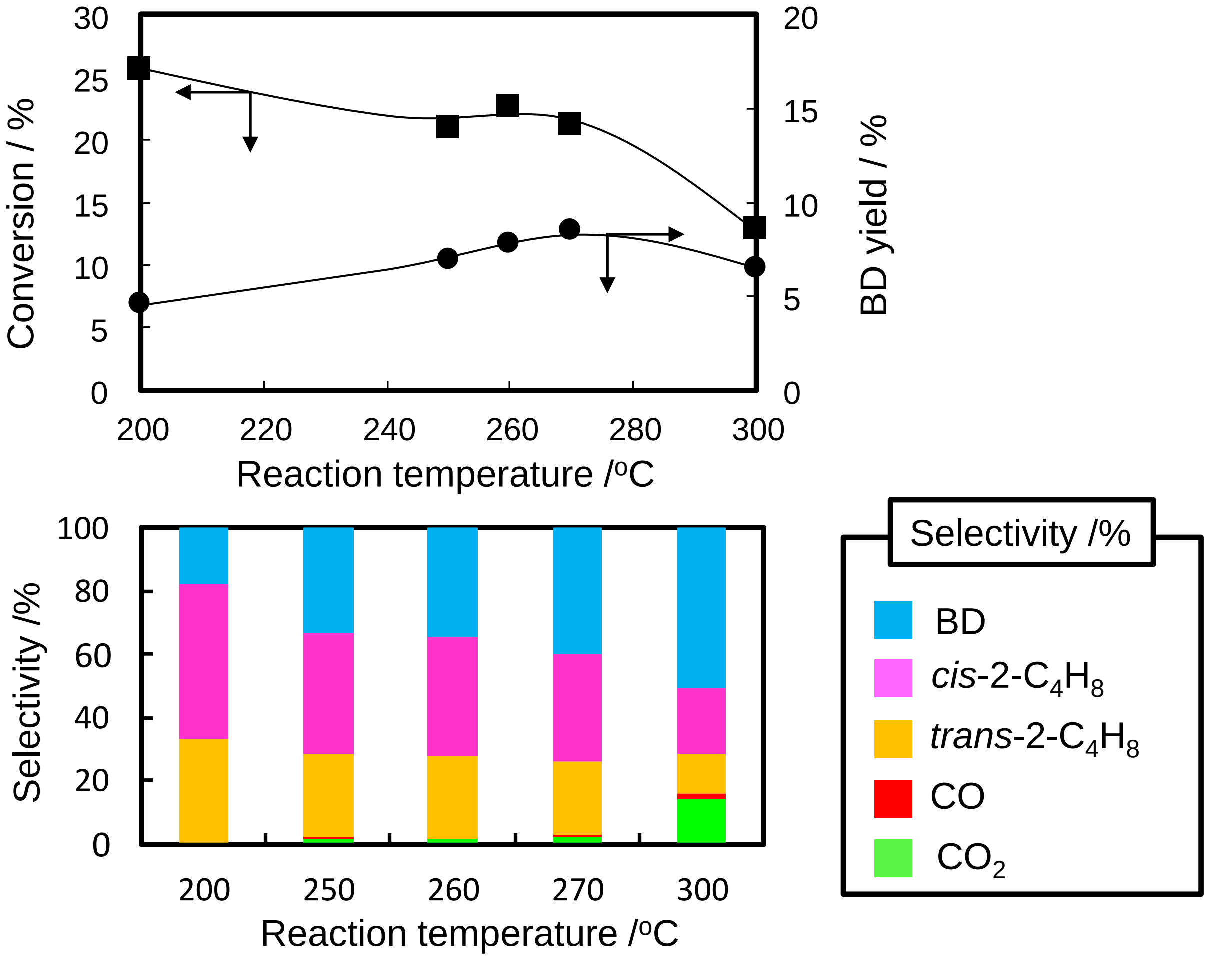

Fig. 2 Oxidative dehydrogenation of but-1-ene with copper ferrite catalyst
Catalyst: $CuFe_2O_4$/AC-500, catalyst weight: 200 mg,
flow rate: 1-$C_4H_8$/Ar=5/25 mL/min, reaction time: 8 min

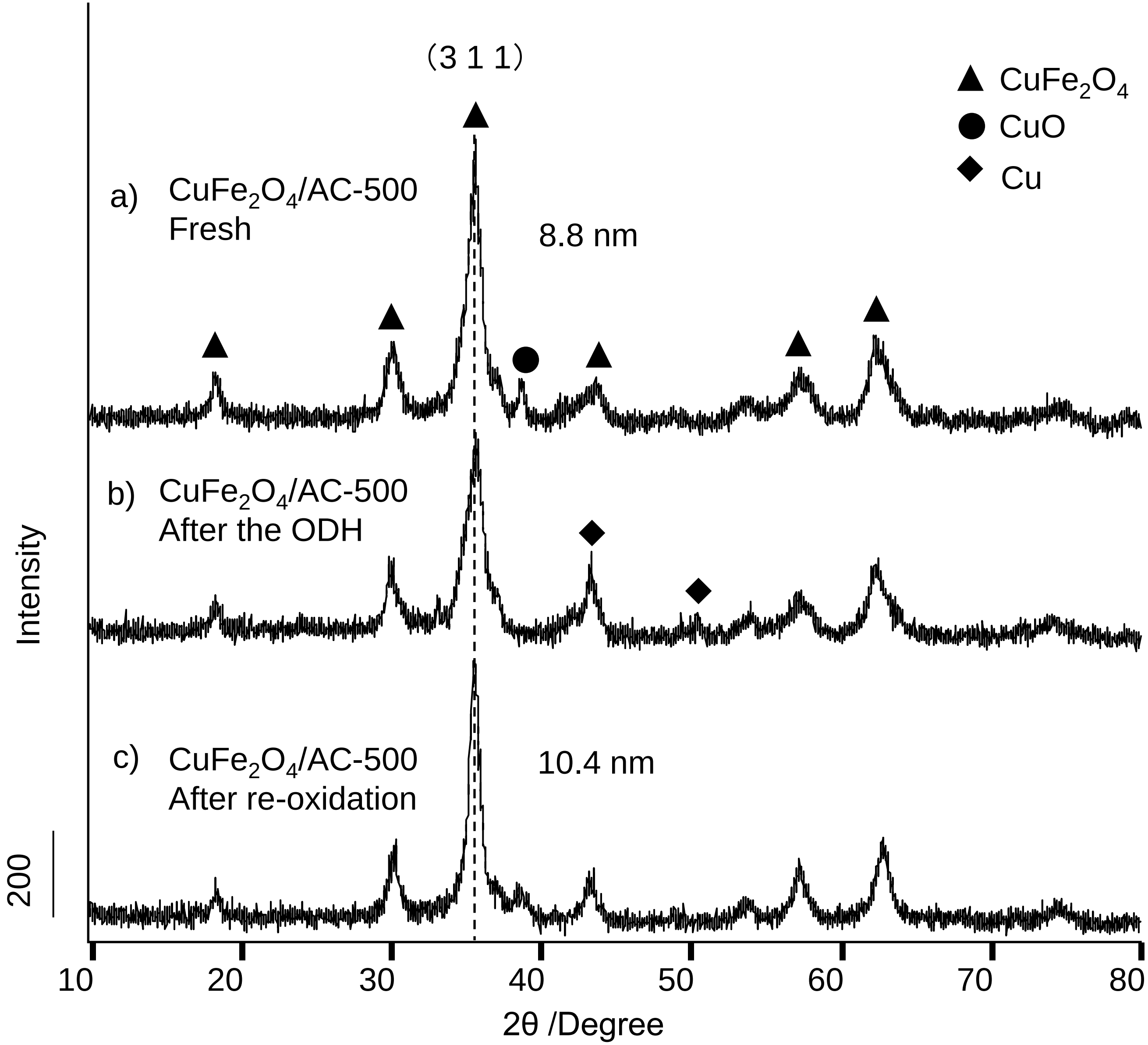

Fig. 3 XRD patterns of copper ferrite after ODH and re-oxidation
a) $CuFe_2O_4$/AC-500 before reaction, b) $CuFe_2O_4$/AC-500 after the ODH at 270 $^oC$,
c) $CuFe_2O_4$/AC-500 after re-oxidation at 270 $^oC$

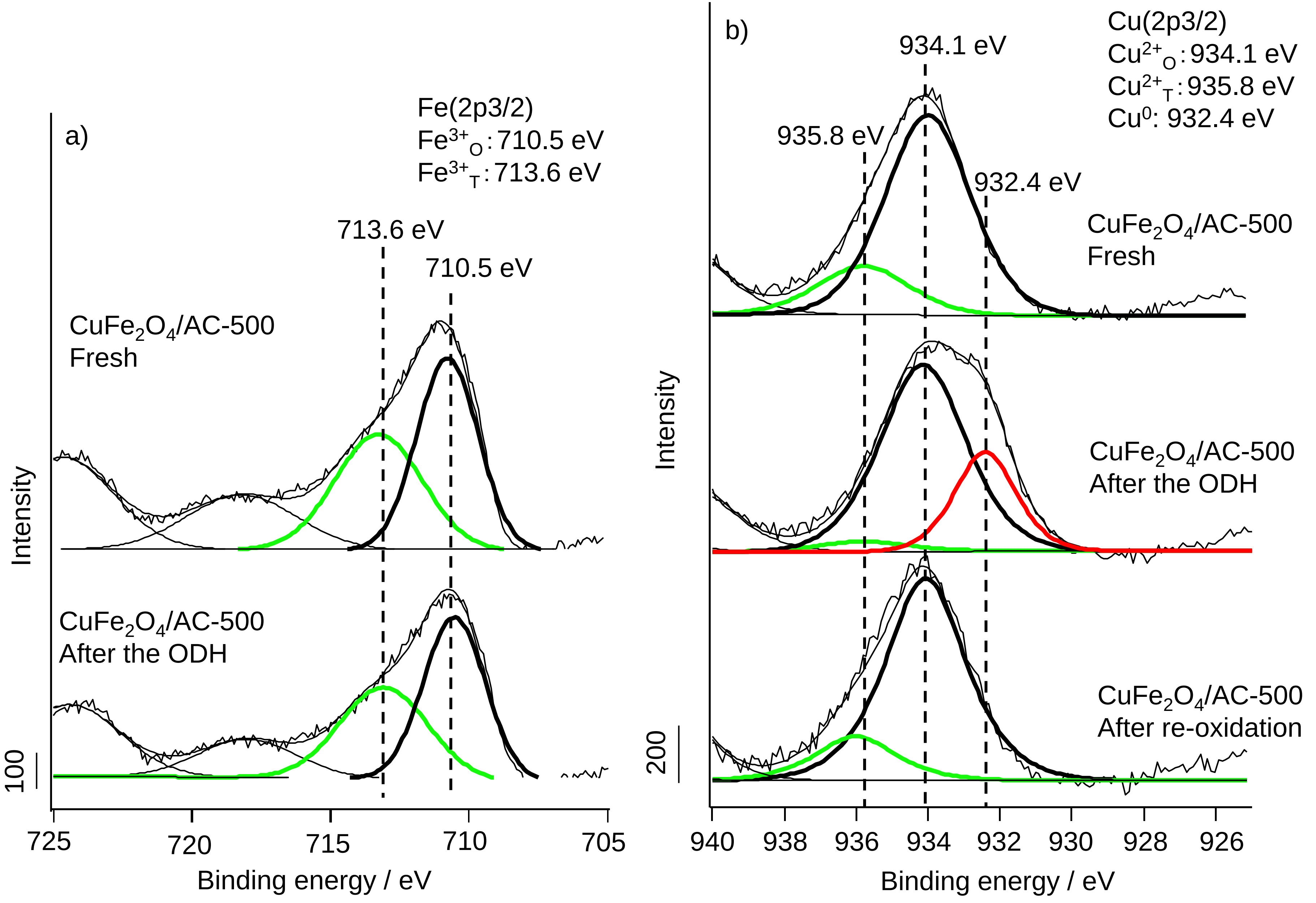

Fig. 4 XPS spectra of $CuFe_2O_4$/AC before and after the ODH and re-oxidation
a) Cu(2p3/2) before and after the ODH and re-oxidation at 270 $^{o}$C, b) Fe (2p3/2) before and after the ODH at 270 $^{o}$C

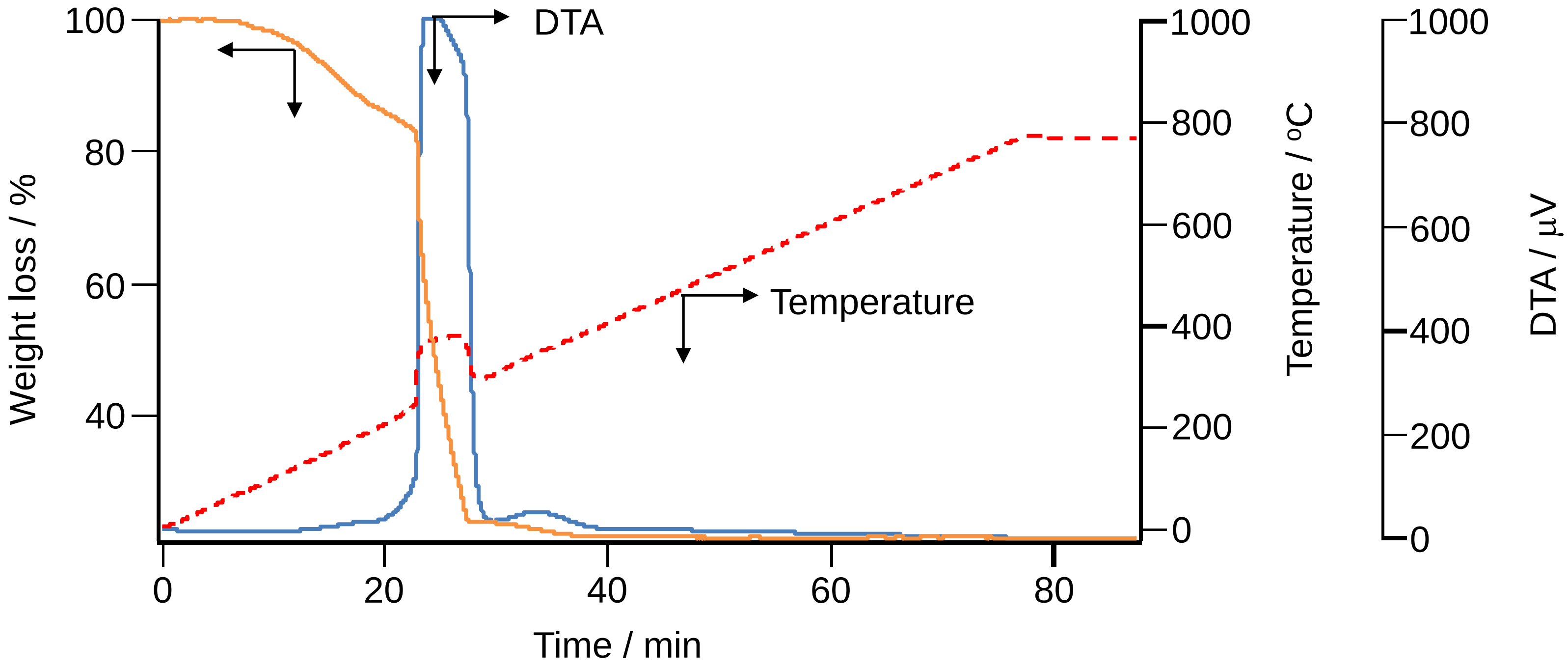

Fig. 5 Weight loss and DTA of copper ferrite before calcination by TG-DTA
Substance: $CuFe_2O_4$/AC before calcination, flow rate: air=100 mL/min,
heating ratio: 5 ºC/min

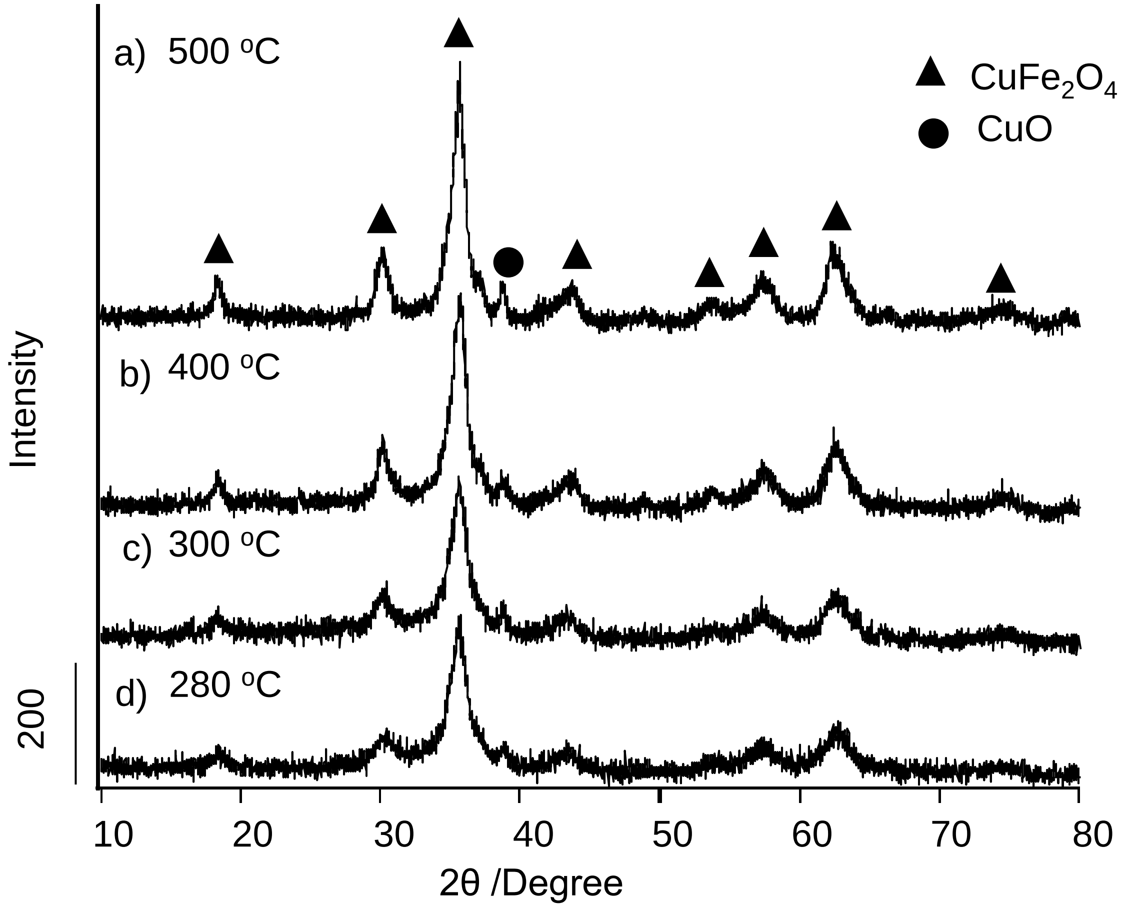

Fig. 6 XRD patterns of copper ferrite calcined at various temperatures
Calcination temp: a) 500 $^{o}$C, b) 400 $^{o}$C, c) 300 $^{o}$C, d) 280
Catalyst notice: a) CuFe2O4/AC-500, b) $CuFe_2O_4$/AC-400, c) $CuFe_2O_4$/AC-300, d) $CuFe_2O_4$/AC-280

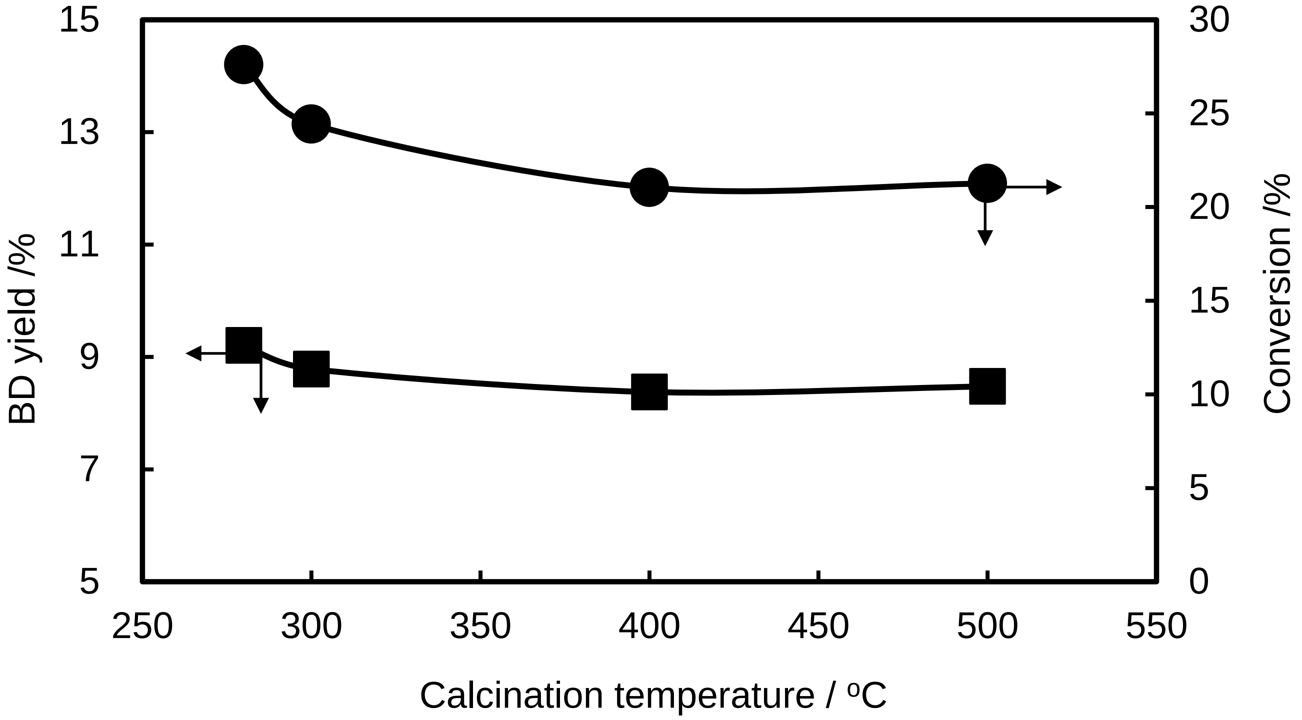

Fig. 7 Effect of calcination temperature on ODH of but-1-ene
Catalyst: $CuFe_2O_4$/AC-500, -400, -300, -280, catalyst weight: 200 mg,
reaction temperature: 270 °C, flow rate: 1-$C_4H_8$/Ar=5/25 mL/min, reaction time: 8 min

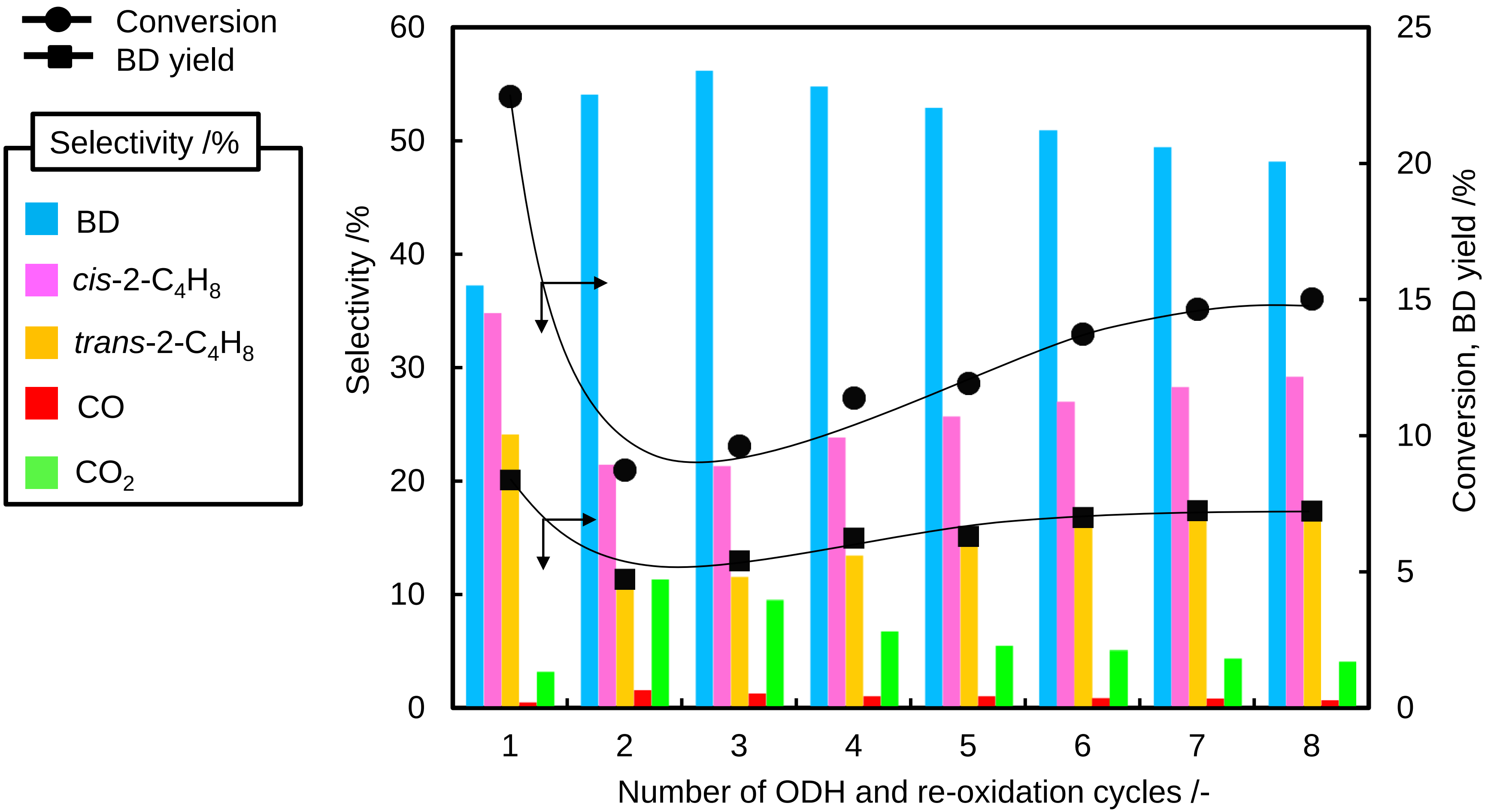

Fig. 8 Repeated ODH of but-1-ene and re-oxidation with $CuFe_2O_4$/AC-500
Catalyst: $CuFe_2O_4$/AC-500, catalyst weight: 200 mg, flow rate: 1-$C_4H_8$/Ar=5/25 mL/min, reaction temperature: 270 °C, reaction time: 8 min, re-oxidation: $O_2$/Ar=5/25 mL/min, re-oxidation temperature: 270 °C, re-oxidation time: 8 min

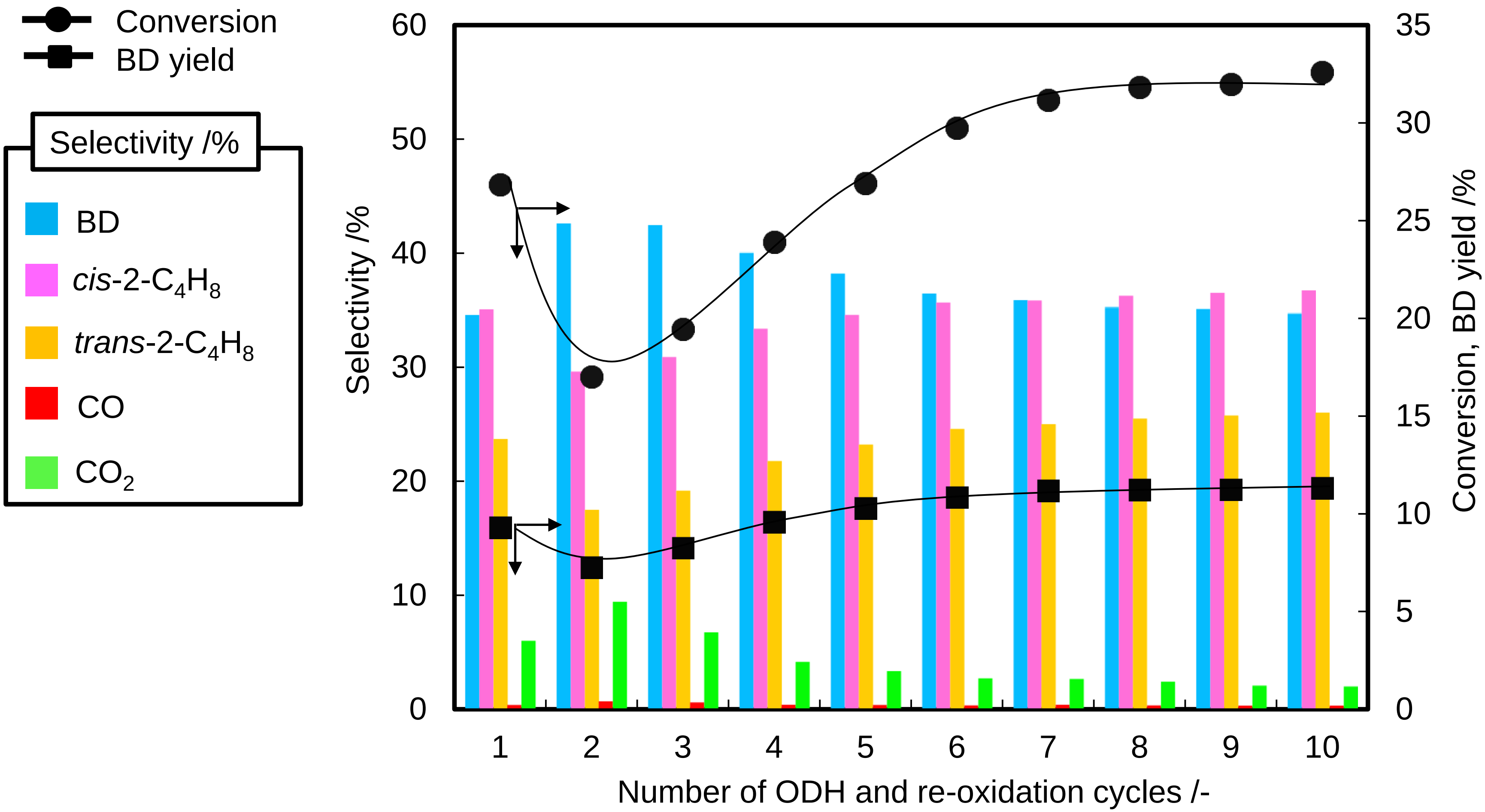

Fig. 9 Repeated ODH of but-1-ene and re-oxidation with $CuFe_2O_4$/AC-280
Catalyst: $CuFe_2O_4$/AC-280, catalyst weight: 200 mg, flow rate: 1-$C_4H_8$/Ar=5/25 mL/min, reaction temperature: 270 $^oC$, reaction time: 8 min, re-oxidation: $O_2$/Ar=5/25 mL/min, re-oxidation temperature: 270 $^oC$, re-oxidation time: 8 min

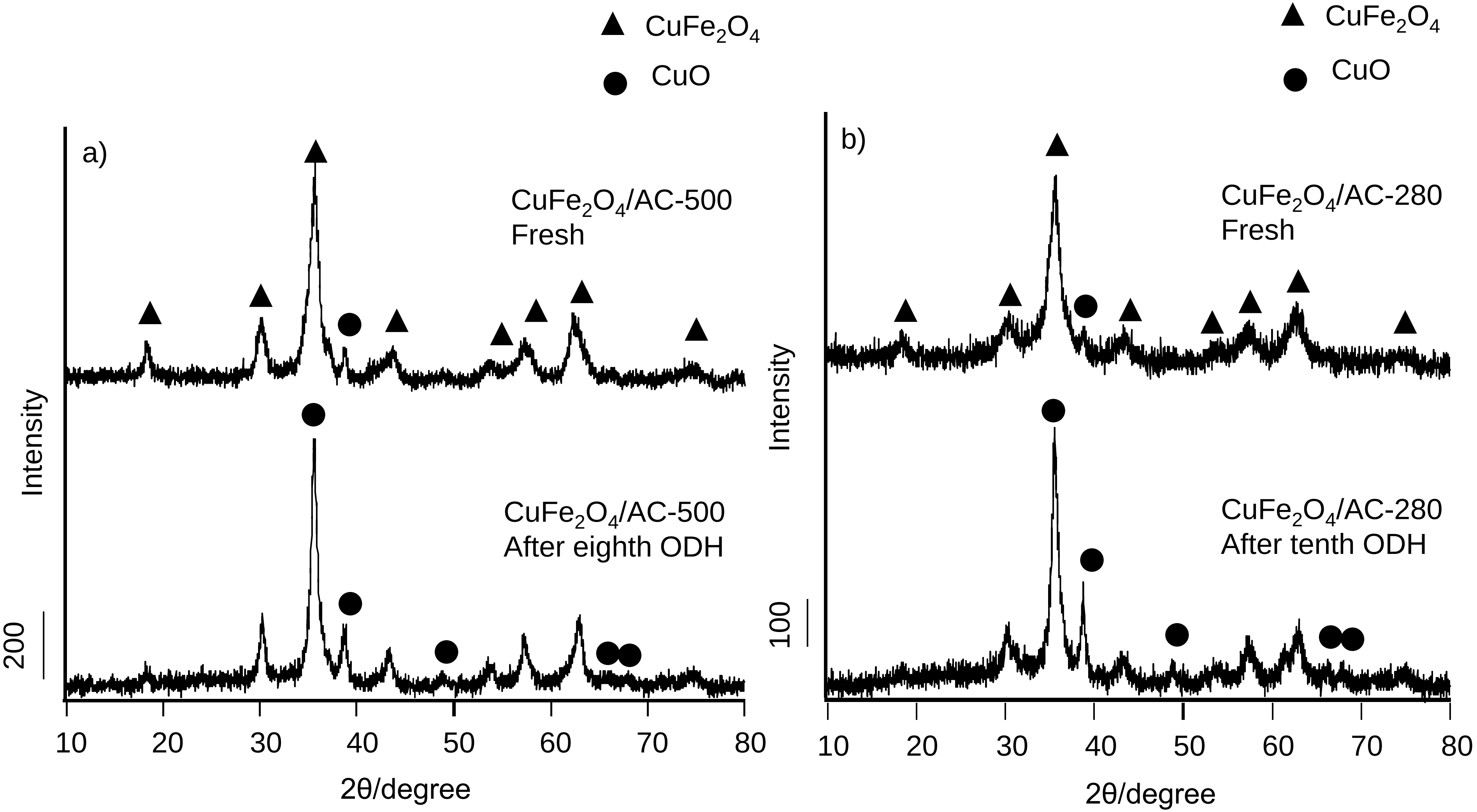

Fig.10 XRD patterns of $CuFe_2O_4$/AC-500 and $CuFe_2O_4$/AC-280 before and after repeatedly ODH
a) $CuFe_2O_4$/AC-500 before and after eighth ODH, b) $CuFe_2O_4$/AC-280 before and after tenth ODH